Experimental Neurology 318 (2019) 258–266

Contents lists available at ScienceDirect

Experimental Neurology

journal homepage: www.elsevier.com/locate/yexnr

Research Paper

GDNF pretreatment overcomes Schwann cell phenotype mismatch to promote motor axon regeneration via sensory graft

Xinyu Fang[1], Chaofan Zhang[1], Zibo Yu, Wenbo Li, Zida Huang, Wenming Zhang*

Department of Orthopedic Surgery, First Affiliated Hospital of Fujian Medical University, Fuzhou, Fujian, China

ABSTRACT

In the clinic, severe motor nerve injury is commonly repaired by autologous sensory nerve bridging, but the ability of Schwann cells (SCs) in sensory nerves to support motor neuron axon growth is poor due to phenotype mismatch. In vitro experiments have demonstrated that sensory-derived SCs overcome phenotypic mismatch-induced growth inhibition after pretreatment with exogenous glial cell-derived neurotrophic factor (GDNF) and induce motor neuron axonal growth. Thus, we introduced a novel staging surgery: In the first stage of surgery, the denervated sensory nerve was pretreated with sustained-release GDNF, which was encapsulated into a self-assembling peptide nanofiber scaffold (SAPNS) RADA-16I in the donor area in vivo. In the second stage of surgery, the pretreated sensory grafts were transplanted to repair motor nerve injury. Motor axon regeneration and remyelination and muscle functional recovery after the second surgery was compared to those in the control groups. The expression of genes previously shown to be differently expressed in motor and sensory SCs was also analyzed in pretreated sensory grafts by qRT-PCR to explore possible changes after exogenous GDNF application. Exogenous GDNF acted directly on the denervated sensory nerve graft in vivo, increasing the expression of endogenous GDNF and sensory SC-derived marker brain-derived neurotrophic factor (BDNF). After transplantation to repair motor nerve injury, exogenous GDNF pretreatment promoted the regeneration and remyelination of proximal motor axons and the recovery of muscle function. Further research into how phenotype, gene expression and changes in neurotrophic factors in SCs are affected by GDNF will help us design more effective methods to treat peripheral nerve injury.

1. Introduction

To improve the repair of severe long segment defects of peripheral nerves (PNs) and promote the recovery of motor function, a variety of treatment methods have been attempted in clinical and experimental research (Eggers et al., 2016; Griffin et al., 2013). In the clinic, PN defects are commonly repaired by autologous neural bridging (Gordon et al., 2011). Motor nerves are rarely used as grafts due to damage to movement function in the donor area. The main source of cells for autologous nerve bridging is sensory nerves. After PN injury, Schwann cells (SCs), the main cellular component of the distal part of the injured PN, are denervated and then dedifferentiated from the mature, myelin phenotype, secreting trophic factors that promote the growth of proximal axons of neurons (Raff et al., 1978). Brushart et al. first proposed the concept of sensory and motor phenotypes of SCs, observing that the axons of motor neurons are more likely to dominate muscles than to dominate skin, which called preferential motor reinnervation (PMR) (Brushart, 1988). Further research found that SCs within the sensory or motor branch of PNs express different factors that promote sensory or motor axon elongation, respectively. If the phenotypes of neurons and SCs do not match, axonal growth will be inhibited (Höke et al., 2006) (Jesuraj et al., 2012). Therefore, when sensory nerve bridging is used to repair long segmental motor nerve defects, the SCs in sensory nerves have a poor ability to support motor neuron axon growth (Brenner et al., 2006; Brushart et al., 2013; Chu et al., 2009; Chu et al., 2008).

Modulating the phenotype and trophic factor secretion of SCs to overcome the influence of phenotypic mismatches is of great significance for improving the efficacy of sensory nerve bridging for repairing motor nerve defects. Studies have found that in the brachial plexus avulsion animal model, glial cell-derived neurotrophic factor (GDNF) is upregulated in the ventral roots after avulsion (Brushart et al., 2013) and promotes motor axon regrowth into the ventral roots (Höke et al., 2003; Höke et al., 2002). In vitro experiments have also demonstrated that sensory-derived SCs overcome phenotypic mismatch-induced growth inhibition after pretreatment with exogenous GDNF and induce motor neuron axonal growth. (Marquardt and Sakiyama-Elbert, 2015). Chu

Abbreviation: PNs, peripheral nerves; SCs, Schwann cells; GDNF, glial cell-derived neurotrophic factor; SAPNS, self-assembling peptide nanofiber scaffold; qRT, quantitative real-time; FG, fluorogold; BDNF, brain-derived neurotrophic factor; NGF, nerve growth factor; PTN, pleiotrophin; IGF-2, insulin-like growth factor; EM, electron microscopy; CMAPs, compound muscle action potentials; PMR, preferential motor reinnervation

* Corresponding author at: Division of Joint Surgery, Department of Orthopedics, First Affiliated Hospital of Fujian Medical University, No. 20 Chazhong Road, Fuzhou 350005, Fujian, China.

E-mail address: zhangwm0591@163.com (W. Zhang).

[1] These authors contributed equally to this work.

https://doi.org/10.1016/j.expneurol.2019.05.011
Received 26 February 2019; Received in revised form 10 May 2019; Accepted 12 May 2019
Available online 14 May 2019
0014-4886/

et al. injected GDNF directly into the transplanted sensory nerve in vivo and found that GDNF promoted more motor neuron axonal regeneration than transplantation of sensory nerves alone (Chu et al., 2009). These studies provide the possibility that exogenous GDNF can be used to pretreat SCs in the sensory nerve to overcome the regrowth inhibition caused by phenotypic mismatch and improve the efficacy of transplantation. However, current studies have not elucidated whether GDNF promotes nerve regeneration in vivo by improving the mismatch between sensory-derived SCs and motor neuron axons. Moreover, in current in vivo studies, GDNF was applied directly to the anastomotic site by injection or gelfoam at the same time as nerve transplantation, causing drug leakage. A high concentration of neurotrophic factor(s) at a leakage area retains the axons and prevents them from growing into the nerves, termed the *candy store* or *growth factor oasis* effect (Blits et al., 2004; Chu et al., 2009).

Based on the above studies, we designed a staging surgery: sensory grafts were pretreated with GDNF in the donor area in vivo and then transplanted to repair motor nerve injury. This approach avoids the adverse effects of direct administration of drugs at the anastomotic sites. Meanwhile, we used a self-assembling peptide nanofiber scaffold (SAPNS) RADA-16I to encapsulate the GDNF for sustained release to avoid drug leakage and loss (Huang et al., 2012; Sun et al., 2016; Zhan et al., 2013). The expression of genes previously shown to be differentially expressed in motor and sensory SCs was also analyzed in pretreated sensory grafts by quantitative real-time (qRT)-PCR to explore possible changes after exogenous GDNF application. We hypothesized that sensory grafts pretreated by this method can overcome the axonal growth inhibition caused by phenotypic mismatch and enhance the regeneration of proximal motor axons and motor functional recovery, potentially attributed to the different expression pattern of phenotype-specific genes.

2. Material and methods

2.1. Animals

All surgical interventions and subsequent care and treatment were approved by the Committee for the Use of Live Animals for Teaching and Research at the First Affiliated Hospital of Fujian Medical University. Animals were provided by the Laboratory Animal Unit at Fujian Medical University.

2.2. Staging animal surgery

Ninety-six female Sprague–Dawley rats (220–250 g) were used in this study. Animals were anesthetized with an intraperitoneal injection of ketamine (80 mg/kg) and xylazine (8 mg/kg) and placed in the supine position. Surgeries were performed in two stages (Fig. 1&2). In the first stage (nerve denervation and pretreatment), animals were randomly divided into four groups: ① GDNF pretreatment (preGDNF) group: The sensory and motor branches of the femoral nerve were both transected at a distance of 5 mm from the bifurcation of the femoral nerve trunk. Two microliters of GDNF (500 ng/μl) was mixed with 13 μl of RADA 16-I solution (BD Biosciences, Cambridge, MA) in a culture dish, and 15 μl of SC culture medium was added and fully mixed into a gelatinous shape to wrap the distal stump of the transected sensory branch. Both the proximal and distal stumps of the transected motor branch were ligated and imbedded into adjacent muscle to prevent regeneration (Fig. 1A). ② Vehicle control (VC) group: In the same way, the sensory and motor branches were transected, and the same medium without GDNF was prepared, mixed with RADA 16-I and adjusted to a gel shape to wrap around the distal stump of the sensory branch (Fig. 1B). ③ Negative control (NC) group: After the same transection procedure, both the proximal and distal stumps of the sensory and motor branch were ligated and imbedded into adjacent muscle to prevent regeneration (Fig. 1C). ④ Positive control (PC) group: Only the motor branch of the femoral nerve was transected at the same site, and both the proximal and distal stumps were ligated and imbedded into adjacent muscle to prevent regeneration (Fig. 1D).

Two weeks later, one-third of the rats in each group ($n = 8$) were killed, and 10 mm of distal nerve segments (the sensory branch for the GDNF, VC, and NC groups and the motor branch for the PC group) were collected for qRT-PCR analysis. The remaining rats received the second stage of the surgery (graft bridging surgery). After anesthesia, a 5-mm nerve segment was taken from the distal part of the sensory branch to bridge the distal and proximal stumps of the motor branch using four 12–0 nylon epineurial sutures for each coaptation in the GDNF, VC and NC groups (Fig. 2A, E, F). In the PC group, a 5-mm nerve segment was cut from the distal part of the motor branch, and then the distal and proximal stumps of the motor branch were bridged by this segment (Fig. 2B).

2.3. qRT-PCR

The expression of genes previously shown to be most obviously differentially expressed in sensory and motor nerves after 2 weeks of denervation in vivo was analyzed by qRT-PCR, including the expression of sensory-derived SC markers, brain-derived neurotrophic factor (BDNF) and nerve growth factor (NGF), and of motor-derived SC markers, pleiotrophin (PTN) and insulin-like growth factor (IGF)-2, as well as the expression of endogenous GDNF (Brushart et al., 2013; Höke et al., 2006). Total RNA was extracted from 10-mm femoral nerve sections (the sensory branch for the GDNF, VC, and NC groups and the motor branch for the PC group, $n = 8$) using TRIzol reagent according to the manufacturer's protocol (Invitrogen, US). The extracted RNA was further purified using DNase-I to eliminate residual genomic DNA. A total of 1 g of total RNA was reverse-transcribed using random primers and reverse transcriptase (M-MLV-RT, Takara, Japan) according to the manufacturer's instructions. qRT-PCR was performed according to standard protocols using SYBR Green Kit (Takara, Japan) in an iCycler iQTM (Bio-Rad).

Briefly, 1 μl of cDNA was added to a 19-μl reaction mixture containing 0.5 μM primer sets and 0.5× SYBR Green mixture. The primers were designed and synthesized by Integrated DNA Technologies (Shatin, N. T., Hong Kong, China). The following primer sequences were used for quantitative real-time PCR: NGF, forward, 5'ACCTCTTC GGACACTCTGGA3'; reverse, 5'GTCCGTGGCTGTGGTCTTAT3'. BDNF, forward, 5' GAACAGGACGGAAACAGAACG3' ; reverse, 5'GAACAGG ACGGAAACAGAACG3' ; GDNF , forward, 5'GCGGTTCCTGTGAAGCG GCCGA3' ; reverse, 5'TAGATACATCCACACCGTTTAGCGG3'; IGF-2 , forward, 5' GAACAACAATAGCCGCCCAAACTC 3' ; reverse, 5' CATG TTCTGTTCCTCTCCTTGGGT 3'; PTN , forward, 5' GCCGAGTGCAAAC AAACCATGAAG 3' ; reverse, 5' AGGCGGTATTGAGGTCACATTCTC 3'; β-actin, forward, 5'-TCATGAAGTGTGACGTGGACATC-3'; reverse, 5' TGTTGCATTTGCGGG GACGATG-3'.

The PCR was run using the following cycling conditions: 95 °C for 5 min and 35 cycles of 95 °C for 30 s, 60 °C for 30 s, and 72 °C for 40 s. The expression level for each myelin gene was calculated as the fold change of the expression in the GDNF-pretreated group compared to that in the VC group using the 2-ΔΔCt method, where ΔCt represents the difference between the Ct values of each gene and β-actin and ΔΔCt represents the difference of ΔCt between the four groups after normalization to β-actin. All PCRs were performed in triplicate and repeated three times.

2.4. Electrophysiological analysis

Twelve weeks after the second stage of surgery (graft bridging), the functional recovery of the quadriceps femoris muscle (QFM) was evaluated by electrophysiological analysis via a standard nerve-evoked potential recording system (RM6240BD, Chengdu, China) in 16 animals per group. The procedure was performed as previously described and

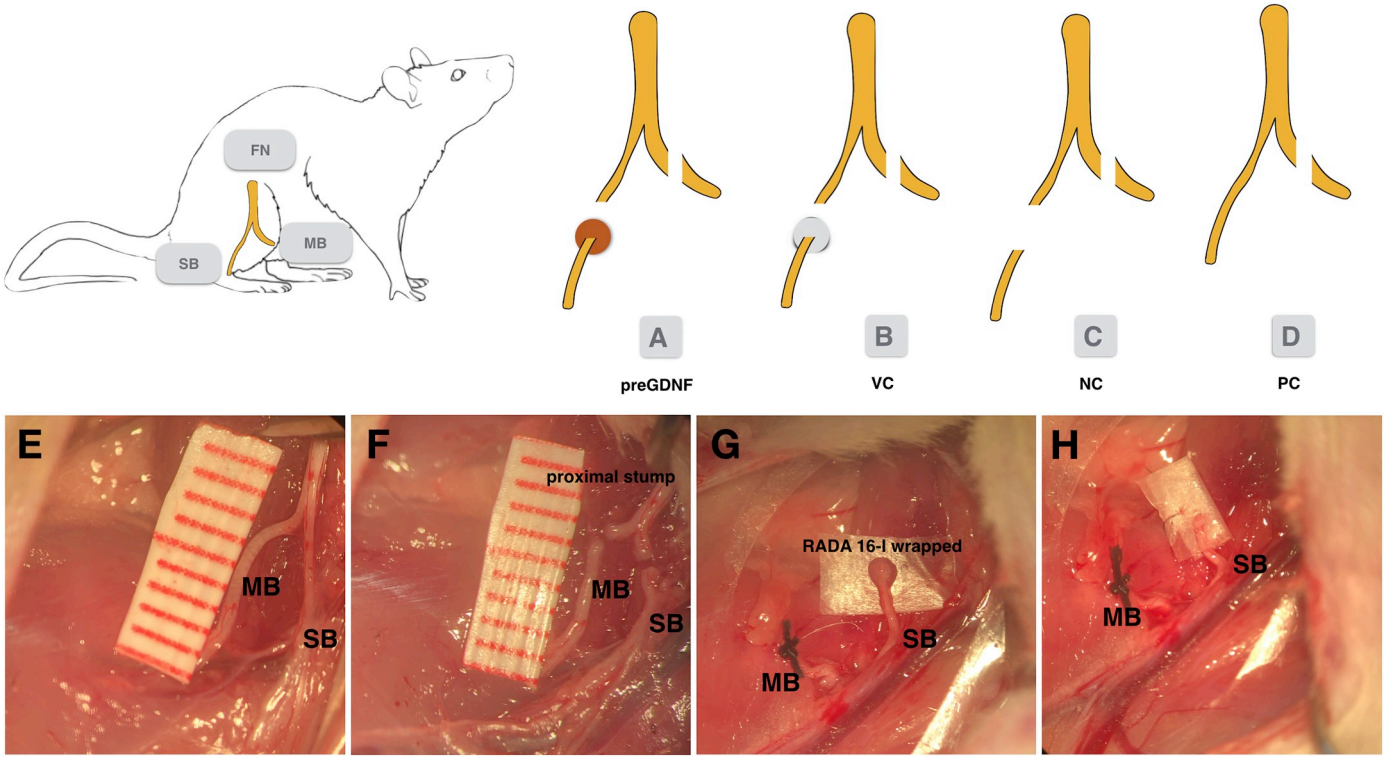

Fig. 1. Schematic photos of nerve denervation and pretreatment surgery (stage I).
(A) preGDNF group: The MB and SB of the FN were both transected. GDNF was mixed with RADA 16-I solution into a gelatinous shape to wrap the distal stump of the transected sensory branch. (B) VC group: The MB and SB of the FN were transected, and the same medium without GDNF was mixed with RADA 16-I into a gelatinous shape, which wrapped the distal stump of the SB. (C) NC group: The same transection procedure was performed without treatment. (D) PC group: Only the MB of the FN was transected at the same site without further treatment. (E) Exposure of the FN and its branches.(F)FB and MB of the FN were transected. (G)RADA 16-I containing GDNF to wrap the distal stump of SB. The distal stump of MB were imbedded into muscle. (H) After gelatinization，the stump was wrapped in parafilm to protect the gel. (FN: femoral nerve; MB: motor branch; SB: sensory branch; preGDNF: GDNF pretreatment; VC: vehicle control; NC: negative control; PC: Positive Control)

illustrated in Fig. 2C(Liu et al., 2013; Zhang et al., 2017). Briefly, animals were anesthetized and placed in a supine position. The resutured motor branch of the femoral nerve and QFM (R) was exposed, and the patellar tendon was transected. The bipolar stimulating electrode was placed underneath the nerve, with which it was kept in contact. The patellar tendon was sutured with 2–0 silk and fixed to a transducer to record muscle contraction force. For recording the compound muscle action potentials (CMAPs), two stainless-steel monopolar recording electrodes were inserted into the muscle belly, and the grounding electrode was inserted into the subcutaneous tissue. An initial electronic electrical stimulus (0.1 mA; 1-ms duration; 1-Hz frequency; square wave) was applied and gradually increased by 0.1 mA until the supramaximal response was reached. The maximum muscle contraction force and evoked CMAP were recorded five times, with 2-minute interstimulus intervals. The same procedure was performed on the contralateral side (L) as a reference. The results are presented as a ratio of the value on the surgical side (R) to that on the contralateral side (L) (R/L) to avoid the influence of individual variation. After electrophysiological analysis, half of the animals were killed with a lethal dose of sodium pentobarbital, perfused intracardially with 0.1 M phosphate buffer (PB) followed by 300 ml 4% paraformaldehyde fixative solution in 0.1 M PB, and prepared for histological analysis. The QFMs were dissected and harvested, and the wet weights of the muscles were measured. The other half of the animals were used for further retrograde axonal tracing procedures.

2.5. Retrograde axonal tracing and FG counting

Twelve weeks after the second stage of surgery (graft bridging surgery), the regeneration of spinal motor neurons into the distal motor branch was examined by retrograde axonal tracing with FG as previously described (Gu et al., 2005) (Fig. 2D) (8 animals per group). Briefly, after exposure of the suture site of the bridging graft, 0.5 μl of 2% (*w/v*) FG solution was injected proximally 10 mm distal to the proximal suture site. The injection lasted 10 s, after which the injection site was clamped with microforceps for 10 s to prevent FG leakage. The rats were maintained for an additional 3 days before sacrifice for evaluation of FG transportation. At the specified time point, rats were perfused and prepared for histological analysis. The L2–4 spinal cord segments were harvested for frozen section examination. Longitudinal sections (30 μm thick) were evaluated to calculate the number of FG-labeled neurons. Images of the right L2–4 ventral horns were captured (100× and 200× magnification) using a fluorescence microscope (Axioplan, Carl Zeiss, Germany). The total numbers of FG-labeled motor neurons in the right L2–4 ventral horn were counted following the previously published methodology (Gu et al., 2005).

2.6. Electron microscopy (EM) analysis

For the EM analysis, after perfusion, the 1-mm segment of graft nerve was harvested after the electrophysiological analysis (8 animals per group). Nerves were processed via the following steps: postfixation in EM fixative (2.5% glutaraldehyde and 2% paraformaldehyde in 0.1 M PB, pH 7.4), osmication in 2% osmic acid, dehydration in increasing concentrations of alcohol (30%–95%), and infiltration and embedding in pure Epon at 60 °C for 3 days. Semithin sections (1 um) were cut using a glass knife in a microtome and were then stained with 0.5% toluidine blue. The data were digitalized by microscopy, and the number of myelinated axons was calculated using ImageJ (US National Institutes of Health, Maryland, USA). Ultrathin sections (80 nm) were

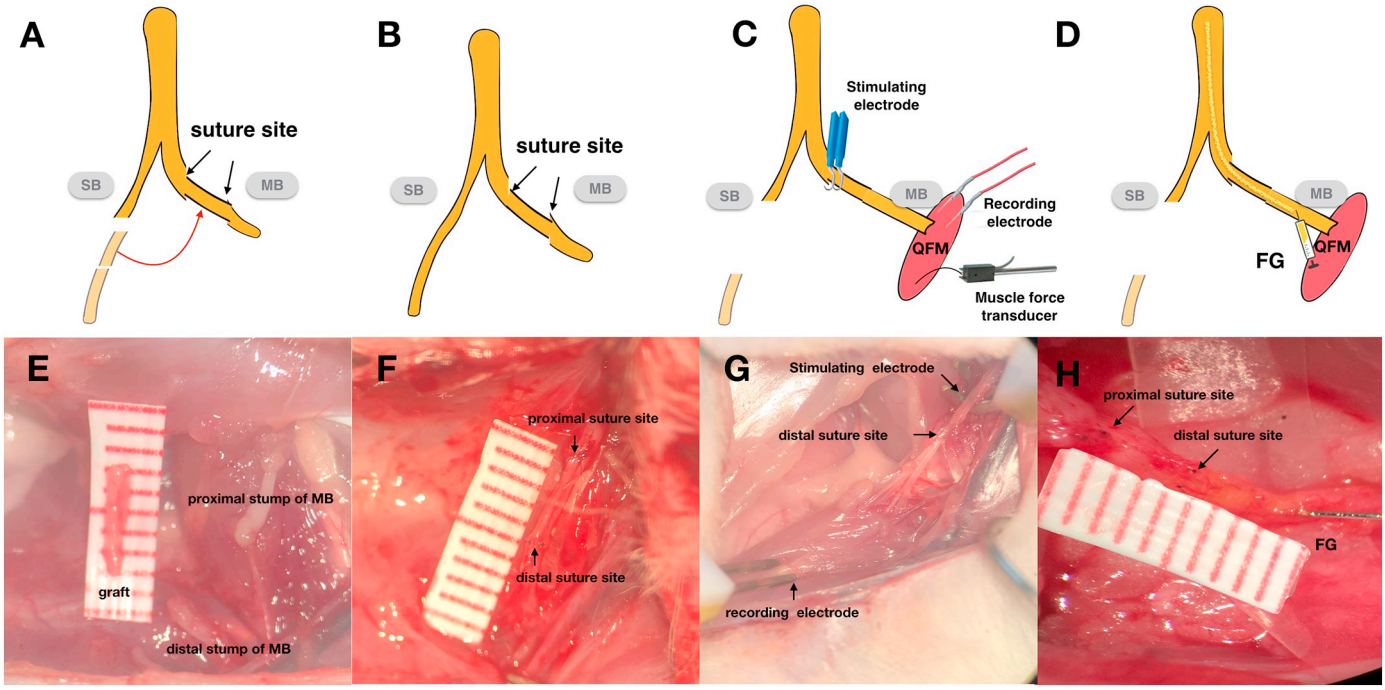

Fig. 2. Schematic photos of graft bridging surgery (stage II), fluorogold (FG) labeling, and electrophysiological analysis.
(A) A 5 mm nerve segment was cut from the distal stump of the SB to bridge the distal and proximal stump ends of the MB in the GDNF, VC and NC groups. (B) For the PC group, the nerve segment was cut from the distal stump of the MB, and then the distal and proximal stumps of the MB were bridged by this segment. (C) Twelve weeks later, electrophysiological analysis was performed. A pair of recording electrodes was inserted into the belly of the QFM, and the bipolar stimulating electrode was placed underneath the nerve proximal to the graft nerve. The patellar tendon was connected to a transducer for detection of the muscle force. (D) FG was injected into the MB 10 mm distal to the proximal suture site of the graft. Motor neurons in the spinal cord that extended axons into the nerve were labeled. (E) The 5 mm nerve segment for graft. (F) Distal and proximal stumps of the MB were bridged by graft using 12–0 suture. (G) The stimulating and recording electrodes were placed for electrophysiological analysis. (H) FG injection site. (FN: femoral nerve; MB: motor branch; SB: sensory branch; NC: negative control; VC: vehicle control; PC: positive control; preGDNF: GDNF pretreatment. QFM: quadriceps femoris muscles; FG: fluorogold).

cut using a diamond knife with an ultramicrotome and collected on 200-mesh copper grids. The sections were stained using drops filtered with 3% lead citrate, followed by 8% (*v*/v) uranyl acetate solutions. Ultrastructural analysis was performed using EM, and the data were digitalized. Myelinated axons in a total of 6 fields (0.5 × 0.5 mm^2) from each animal (8 animals per group) were randomly selected. The G-ratio, which was calculated by dividing the inner diameter of the axon (without myelin) by the outer diameter of the entire fiber (including the myelin), was calculated using Image J to evaluate the myelination of regenerating axons. At least 100 myelinated axons were randomly selected for calculation in each animal. The count of myelinated axons and the calculation of G-ratio were performed.

2.7. Statistical analysis

Imaging analyses were evaluated in a blinded manner. Sections were randomly assigned identification numbers, and two experienced investigators (X Fang and C Zhang) respectively assessed the slides. The values were averaged before further analysis. All the data was presented as the means ± SD. Statistical significance was assessed using a one-way ANOVA followed by a post hoc Dunnett's test for multiple comparisons in SPSS 13.0 (Chicago, IL). *P* values < .05 were considered significant.

3. Results

3.1. Enhanced expression of endogenous GDNF and sensory-derived SC markers in GDNF-pretreated sensory grafts

Two weeks after the first stage (nerve denervation and pretreatment) of surgery, the expression of sensory-derived SC markers (BDNF and NGF), motor-derived SC markers (PTN and IGF-2) and endogenous GDNF was measured by qRT-PCR (Fig. 3). The expression of PTN and IGF-2 (motor markers) in the preGDNF group was not significantly different from that in the NC and VC groups (Fig. 3A&B, $P > .05$) and was significantly lower than that in the PC group (3A&B, $\Delta P < .05$ compared with the PC group), showing that GDNF did not change the expression of motor-derived SC markers in the denervated sensory nerve. Consistent with previous studies, the expression of BDNF and NGF (sensory markers) in the denervated sensory nerve (the PC, VC and preGDNF groups) was higher than that in the denervated motor nerve (the PC group) (Fig. 3C&D, $\Delta P < .05$ compared with the PC group). BDNF expression in the GDNF-pretreated sensory nerves (preGDNF group) was 2.3-fold and 2.5-fold higher than the expression in the untreated sensory nerves (NC and VC groups, respectively), showing statistically significant differences (Fig. 3C, * $P < .05$ compared with the NC group, #$P < .05$ compared with the VC group). Although the expression level of NGF in the preGDNF group reached 1.4-fold that in the NC and VC groups, the difference was not statistically significant (Fig. 3D, $P > .05$). Furthermore, the expression of endogenous GDNF in the preGDNF group was significantly increased, reaching 4.4-fold and 3.1-fold that in the NC group and VC group, respectively (Fig. 3E, * $P < .05$ compared with the NC group, #$P < .05$ compared with the VC group $P < .05$), and close to the expression level in the PC group (Fig. 3E, $P > .05$).

3.2. GDNF-pretreated sensory grafts promoted axonal regeneration of motor neurons after the second stage of surgery

Twelve weeks after the second stage of surgery, neurons labeled with FG were concentrated in the ventral horn of the lumbar 2–4 segment (Fig. 2, A-D). Counting the FG-labeled motor neurons showed that

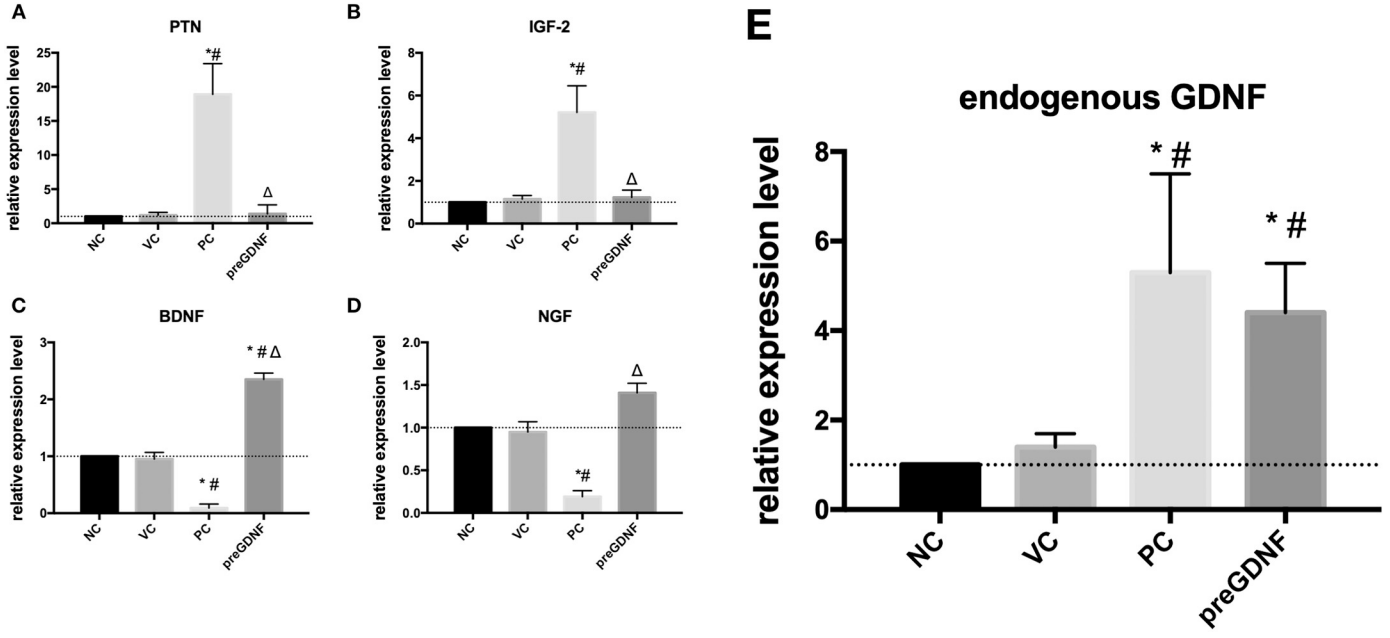

Fig. 3. Phenotypic marker expression change in the sensory branch of the femoral nerve after GDNF pretreatment.
The expression patterns of PTN (A) and IGF-2 (B) (motor markers), BDNF (C) and NGF (D) (sensory markers) and endogenous GDNF was analyzed by qRT-PCR 2 weeks after nerve denervation. The fold difference in gene expression in different groups was compared to the expression in the NC group, and the expression level in the NC group was normalized to 1 arbitrary unit. The expression of PTN and IGF-2 (motor markers) in the preGDNF group was not significantly different from that in the NC and VC groups and was significantly lower than that in the PC group. The expression of BDNF (sensory marker) in the preGDNF group was significantly higher than that in the NC and VC groups. Although the expression of NGF in the preGDNF group was higher than that in the NC and VC groups, the difference was not significant. The expression of endogenous GDNF in the preGDNF group was significantly higher than the expression in the NC group and the VC group. The dotted line at 1 represents similar expression to the NC group. Error bars represent the standard deviation ($n = 8$). * $P < .05$ compared with the NC group, # $P < .05$ compared with the VC group, Δ $P < .05$ compared with the PC group. (NC: negative control; VC: vehicle control; PC: positive control; preGDNF: GDNF pretreatment; PTN: pleiotrophin; IGF-2: insulin-like growth factor 2; BDNF: brain-derived growth factor; NGF: nerve growth factor).

the numbers of motor neurons in the lumbar 2–4 segment in the NC group (Fig. 4A), VC group (Fig. 4B), PC group (Fig. 4C), and preGDNF group (Fig. 4D) were 394.6 ± 92.1, 385.8 ± 79.1, 602.3 ± 66.1 and 526.4 ± 65.2, respectively. Although the number of FG-positive motor neurons in the preGDNF group was less than that in the PC group, the difference was not significant (Fig. 4E, $P > .05$). The number of FG-positive neurons in both the preGDNF and PC groups was significantly higher than that in the NC group and VC group, showed that motor neuron in preGDNF group generated more axon into distal nerve (Fig. 4E, * $P < .05$ compared with the NC group, #P < .05 compared with the VC group).

3.3. GDNF-pretreated sensory grafts promoted remyelination of regenerating motor axons after the second stage of surgery

Twelve weeks after the second stage of surgery, semithin sections of the grafts of each group showed that the numbers of myelinated nerve fibers in the NC group (Fig. 5A), VC group (Fig. 5B), PC group (Fig. 5C) and preGDNF group (Fig. 5D) were 437.1 ± 133.5, 416.3 ± 101.3, 647.9 ± 133.6, and 625.3 ± 106.8, respectively. There was no significant difference in the number of myelinated nerve fibers between the preGDNF group and the PC group (Fig. 5E, P > .05), and the preGDNF group had significantly more myelinated nerve fibers than the NC group and the VC group (Fig. 5E, * compared with the NC group, $P < .05$, # compared with the VC group, P < .05). EM ultrathin sections of the grafts of each group were used to calculate the G-ratio of the myelinated nerve fibers (axonal diameter/total length of the myelin sheath). The G-ratios in the NC group (Fig. 5F), VC group (Fig. 5G), PC group (Fig. 5H) and preGDNF group (Fig. 5I) were 0.706 ± 0.117, 0.729 ± 0.105, 0.410 ± 0.101, and 0.554 ± 0.125 respectively (Fig. 5J). The G-ratio in the preGDNF group was significantly higher than that in the PC group (Fig. 5 J, Δ compared with the PC group, $P < .05$) and significantly lower than those in the NC group and VC group (Fig. 5 J, * compared with the NC group, P < .05, # compared with the VC group, P < .05), indicating that the myelin sheath thickness of the myelinated nerve fibers in the preGDNF group was thicker than those in the NC and VC groups but thinner than that in the PC group.

3.4. GDNF-pretreated sensory grafts promoted electrophysiological functional recovery of muscle after the second stage of surgery

At 12 weeks after nerve bridging, the muscles of each group were significantly atrophied compared with those on the contralateral side, but the degree of atrophy in the preGDNF group and the PC group was alleviated compared to that in the NC group and VC group (Fig. 6A). The wet weight R/L ratios of the quadriceps muscles in the NC group, VC group, PC group and preGDNF group were 0.42 ± 0.18, 0.43 ± 0.11, 0.77 ± 0.17, and 0.61 ± 0.12, respectively. The wet weight of the preGDNF group was lower than that of the PC group (Fig. 6B, Δ compared with the PC group, P < .05) but higher than those of the other two groups (Fig. 6B, * P < .05 compared with the NC group, # P < .05 compared with the VC group). These results indicate that sensory nerve transplantation after GDNF treatment promotes axon growth and myelination which reduces muscle atrophy on the injured side. Electrophysiological methods were used to detect the redistribution of nerves to muscles. The nerve conduction test (NCS) showed that the preGDNF group had a larger CMAP and greater muscle contractility force than the two control groups (Fig. 6 G&H, * P < .05 compared with the NC group, # P < .05 compared with the VC group), but these values were smaller than those in the PC group (Fig. 6 G&H, Δ P < .05 compared with the PC group).

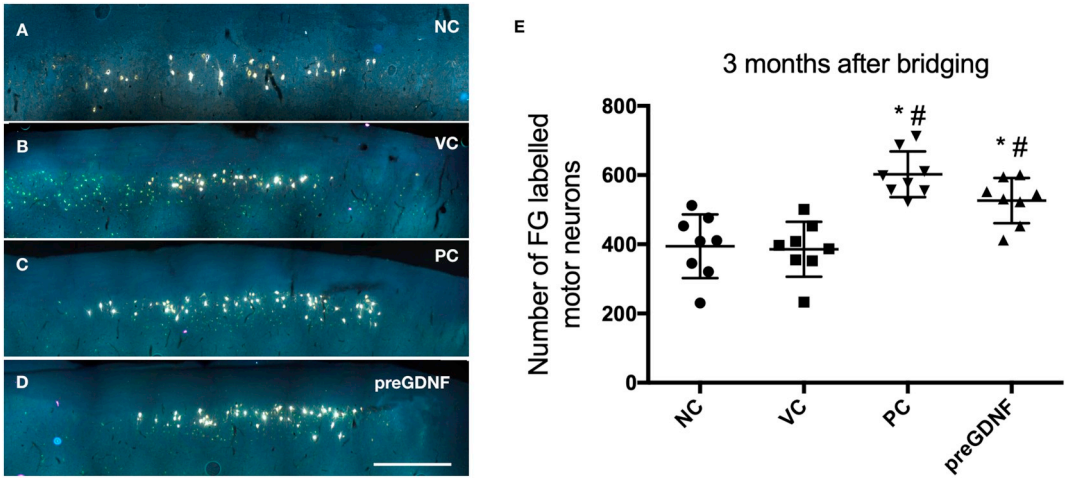

Fig. 4. FG labeling of motor neurons in the spinal cord 12 weeks after the second stage of surgery.
Representative images of FG-labeled motor neurons in the longitudinal sections of the L2–4 ventral horn in the NC group (A), the VC group (B), and the PC group (C), the preGDNF group (D) (scale bar = 100 μm). The number of FG-labeled motor neurons in the preGDNF group was significantly higher than that in the NC group and the VC group, and there was no significant difference from that in the PC group. Error bars represent the standard deviation (n = 8). * P < .05 compared with the NC group, # P < .05 compared with the VC group, Δ P < .05 compared with the PC group. (NC: negative control; VC: vehicle control; PC: positive control; preGDNF: GDNF pretreatment).

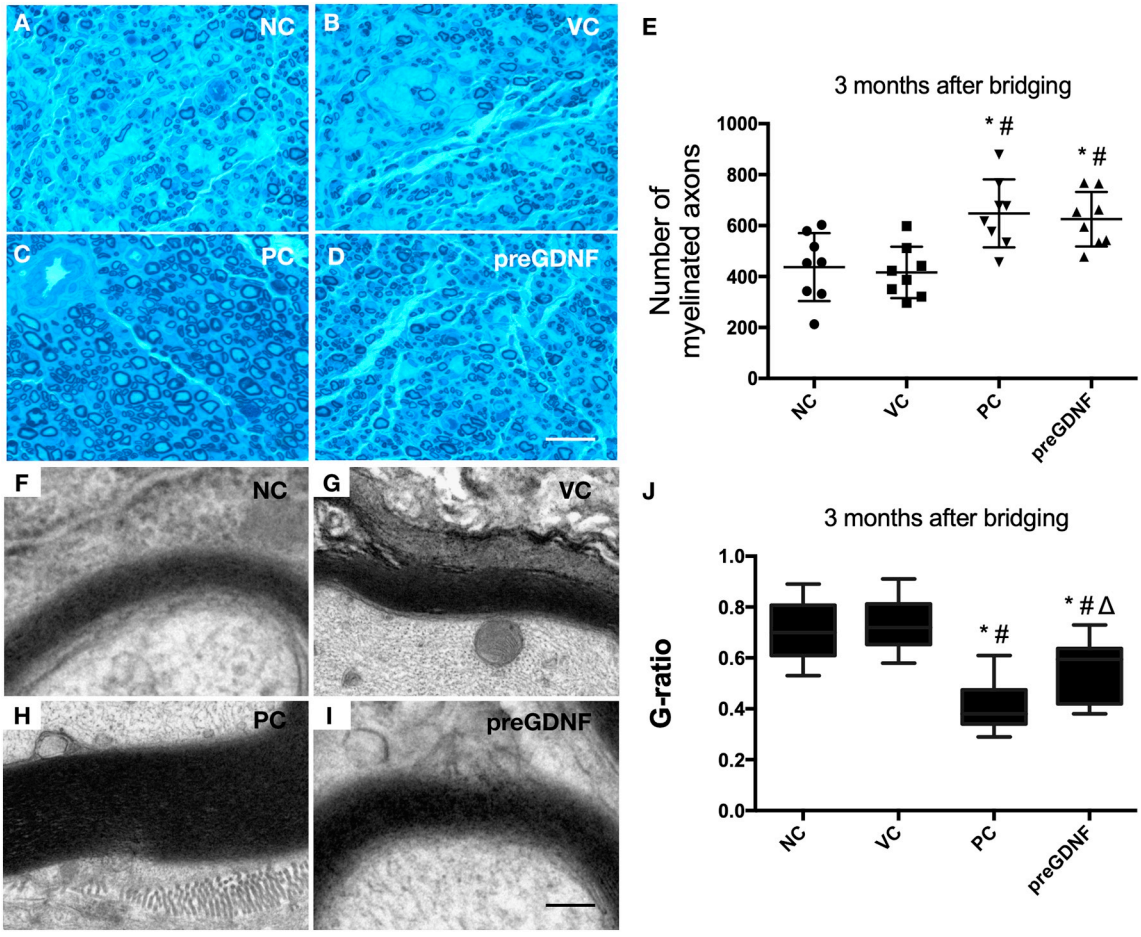

Fig. 5. Comparison of regenerating myelinated axons in each group 12 weeks after the second stage of surgery.
Representative images of semithin sections (toluidine blue staining, scale bar = 100 um) and ultrathin sections (lead citrate and uranyl acetate staining, scale bar = 500 nm) of the rebridged nerve in the NC group (A, F), VC group (B, G), PC group (C, H), and preGDNF group (D, I). (E) The number of myelinated axons in the preGDNF group was significantly higher than those in the NC group and VC group but not significantly different from that in the PC group (J). The G-ratio in the preGDNF group was significantly higher than that in the PC group and significantly lower than those in the NC group and VC group. Error bars represent the standard deviation (n = 8). * P < .05 compared with the NC group, # P < .05 compared with the VC group, Δ P < .05 compared with the PC group. (NC: negative control; VC: vehicle control; PC: positive control; preGDNF: GDNF pretreatment). (For interpretation of the references to colour in this figure legend, the reader is referred to the web version of this article.)

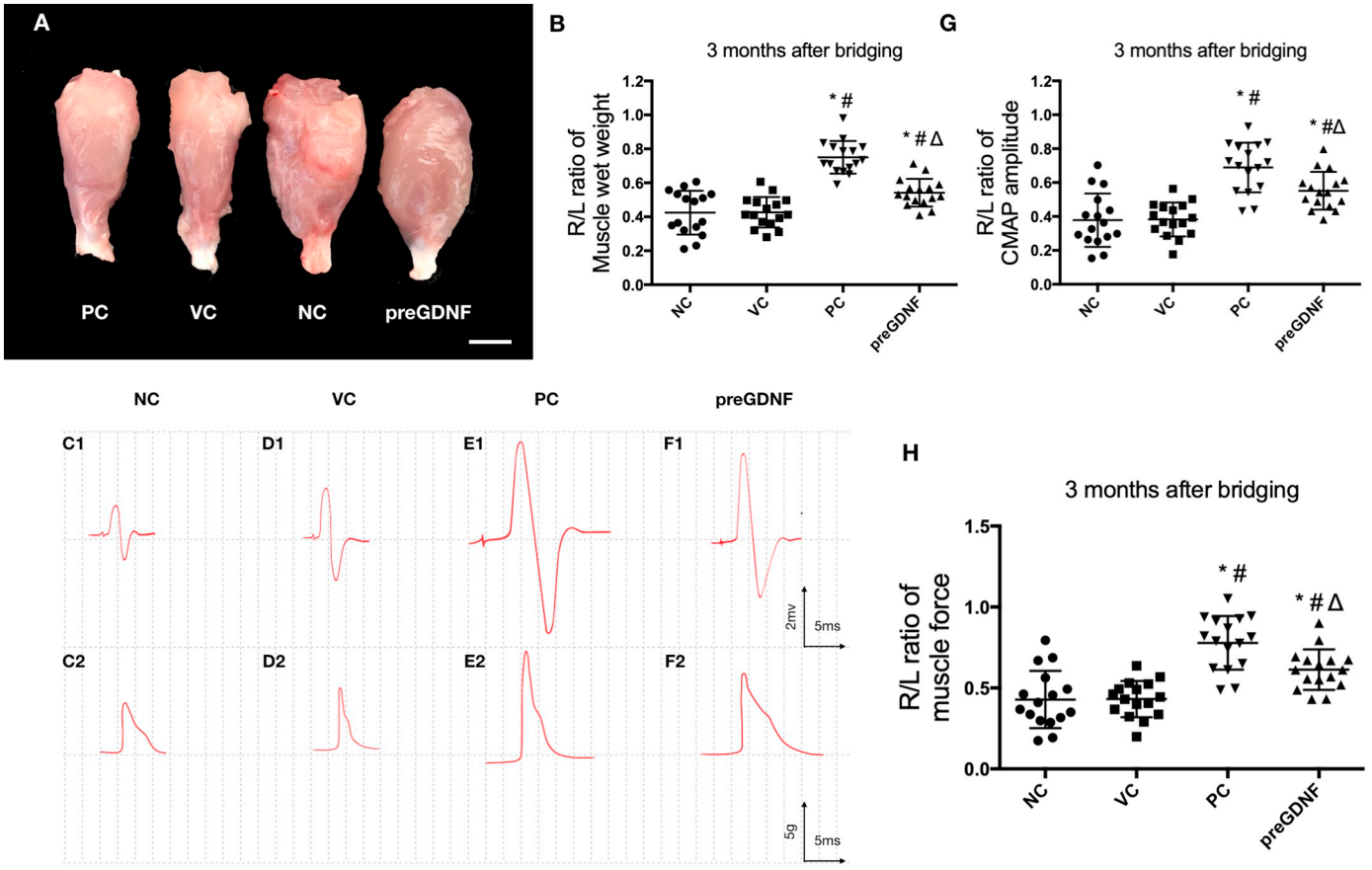

Fig. 6. Comparison of atrophy and electrophysiological function of quadriceps muscles in each group 12 weeks after the second stage of surgery.
Representative images of the general appearance (A, Scale bar = 5 mm) and stimulation-induced action potential of the NC (C1–2), VC (D1–2), PC (E1–2) and the preGDNF (F1–2) group. (B) The wet weight of the preGDNF group was significantly lower than that of the PC group but significantly higher than that of the other two groups. (G, H) The preGDNF group had significantly greater CMAP and greater muscle force than the two control groups but lower than the PC group. * $P < .05$ compared with the NC group, # $P < .05$ compared with the VC group, Δ $P < .05$ compared with the PC group. (NC: negative control; VC: vehicle control; PC: positive control; preGDNF: GDNF pretreatment; CMAPs: compound muscle action potentials).

4. Discussion

The current methods for repairing nerve defects include the use of tissue engineering materials combined with cell transplantation, allogeneic nerve transplantation, autologous nerve transplantation, etc. (Hu et al., 2007; Lohmeyer et al., 2009; Xue et al., 2012). There are still many problems associated with the use of bioscaffolds and allogeneic nerve grafting techniques, such as transplanted immune rejection, cell source and ethics, and poor regeneration, which limit its application (Griffin et al., 2013; Kehoe et al., 2012). Autologous sensory nerve transplantation is a commonly used repair method in the clinic that may be more feasible than the above methods. However, the efficacy of autologous nerve transplantation is still unsatisfactory. The mismatch between SCs and neuron phenotype may be an important factor. Therefore, based on previous studies in vitro, this study aimed to examine the interaction between SCs and motor neurons in autologous sensory nerves in vivo and then use a suitable method to create an environment conducive to motor axon growth, potentially improving the efficacy of autologous nerve transplantation. After pretreatment of the sensory nerves by our methods, proximal motor axon regeneration and remyelination were promoted, the electrophysiological function of the reinnervated muscles was improved, and muscle atrophy was alleviated.

When repairing nerve defects with grafts, the delivery of growth factors to the repair site is a common method used to guide the regeneration of axons across a nerve defect (Marquardt et al., 2015; Wood et al., 2009) In our previous studies, we injected neurotrophic factors directly into the transplanted sensory nerves to compensate for the lack of sufficient trophic factors to induce motor axon growth and showed that GDNF is a more effective factor than other factors tested. Therefore, the GDNF concentration used in previous studies was also used in this study. However, directly injected GDNF could not be accurately maintained in the transplanted nerve, often leaking to the surrounding tissue making it insufficiently effective, and the regenerated axon grew in a disorderly fashion in the leakage site and could not accurately enter the transplanted nerve. As a new type of nanomaterial, SAPNS has been proven to be superior to other materials in tissue repair, due to characteristics such as the ability to minimize the risk of carrying pathogens, create a three-dimensional environment suitable for cell growth, be nontoxic to the host, and induce no obvious immune response. SAPNS easily adapts to various shapes of the damaged environment, immediately stops bleeding, releases the drug slowly, and requires a significantly lower dosage than oral administration or injection [19–26, 33, 34]. This method has been used for administration in central nervous system injury, such as injury in the brain and spinal cord, and proven to result in sustained release and minimal leakage (Guo et al., 2009; Koutsopoulos et al., 2009). In this experiment, RADA-16I-coated GDNF sustained-release administration was used to pretreat the transected sensory nerve followed by transplantation 2 weeks later, thereby avoiding the adverse effects caused by direct administration at the nerve transplantation site (Blits et al., 2004; Chu et al., 2009). Denervation and pretreatment of the distal nerve for 2 weeks also provides some advantages, including activation of SCs and secretion of neurotrophic factors, which peaks after 2 weeks of denervation, leading to the

promotion of axonal regeneration (Jonsson et al., 2013; Michalski et al., 2008). Moreover, because most clinical nerve repairs are performed several weeks after the injury to avoid acute inflammation, delayed repair is more in line with clinical practice.

To explore the possible mechanism by which exogenous GDNF-pretreated sensory grafts promote motor axon growth, the expression of genes previously shown to be obviously differentially expressed between sensory and motor nerve denervation in vivo was analyzed by qRT-PCR, including sensory-derived SC markers BDNF and NGF and motor-derived SC markers PTN and IGF-2 (Brushart et al., 2013; Höke et al., 2006). The expression of motor-derived SC markers (PTN and IGF-2) in the sensory nerve was not enhanced after pretreatment. In contrast the expression of the sensory-derived SC markers BDNF and NGF was enhanced by GDNF pretreatment, although the difference in NGF expression was not significant. Interestingly, in an in vitro experiment performed by Jesuraj, exogenous GDNF also promoted native phenotypic marker expression in femoral sensory and motor-derived SC culture; although the marker examined was different, the trend of the experimental results was consistent with our data (Jesuraj et al., 2014). If the role of GDNF is simply to induce the original muscle-derived and sensory-derived SCs further into their distinct phenotypes, such aggravated mismatches may theoretically inhibit the growth of motor axons, but the opposite is true. To further study the mechanism by which exogenous GDNF promotes axon growth, we detected the expression of endogenous GDNF in sensory grafts after pretreatment and observed that the expression level of endogenous GDNF was obviously increased, even to levels close to the level in motor grafts, consistent with the in vitro results of Marquardt (Marquardt and Sakiyama-Elbert, 2015). The GDNF pathway in SCs has been shown to involve a positive feedback system through activation of the Mek/Erk pathway, potentially explaining the increase in endogenous GDNF expression observed in our results (Iwase et al., 2005). As both motor and sensory neurons respond to GDNF (Gordon, 2014), an overall increase in GDNF in the system may cause axonal extension to overcome growth inhibition. Although BDNF is a marker of sensory-derived SCs, it promotes the regeneration of peripheral nerve axons (Gao et al., 2016), which may promote motor axon regeneration. Pretreatment with GDNF not only promoted axon growth but also enhanced motor axon remyelination, potentially due to an increase in the interaction between the regenerated motor axons and the pretreated SCs in the sensory graft or an increase in the expression of GDNF or BDNF, which directly enhances the role of SCs in remyelination after nerve injury (de Groot et al., 2006; Rosenberg et al., 2006; Zhang et al., 2009).

Previous studies have suggested that short femoral nerve grafts do not exhibit PMR effects, but the difference is that these studies used fresh nerve segments for transplantation (Kawamura et al., 2010; Neubauer et al., 2010), and a pre-degeneration of graft and distal motor nerve was performed in our study. Other studies have also found that the use of pre-degeneration models may enhance the effects of PMR (Abdullah et al., 2013). This may be related to The upregulate of laminin and growth factors in denervated SCs reaches a peak after two weeks of pre-degeneration, which may enhance regeneration and the PMR effects (Abdullah et al., 2013; Brushart et al., 2013; Höke et al., 2006; Wallquist et al., 2004). Meanwhile, myelin-Associated glycoprotein (MAG), an inhibitor of regeneration and PMR, is cleared from the distal stump by Wallerian degeneration and can no longer be detected 1 week after injury (Mears et al., 2003; Schäfer et al., 1996). In combination with the pre-degeneration and pretreatment of GDNF, the sensory graft may be brought to a better state for transplantation.

In peripheral nerve injury in which the injury site is far from the target organ (muscle or skin), such as brachial plexus injury (Fang et al., 2016; Griffin et al., 2013), the SCs in the nerve may play an important role in axon regeneration. Therefore, this study focused on the regulation of SCs in grafts, but the mechanisms leading to the change in expression of sensory and motor-derived SC markers after GDNF treatment still need to be further clarified. Moreover, studies have also noted that in the absence of SCs at the distal stump of the nerve, the motor axons can still regenerate in the direction of the muscle, whereas if there is no muscle at the distal end and only a muscle nerve branch, motor axon regeneration is more limited, indicating that the muscle is also an important inducer of axon regeneration (Madison et al., 2009). Therefore, this study is limited as it did not examine the effect of the target organ on regeneration, which requires further investigation.

5. Conclusion

We concluded from this study that exogenous GDNF acts directly on the sensory nerve graft in vivo, increasing the expression of endogenous GDNF and the sensory SCs-derived marker BDNF, which promotes the regeneration and remyelination of proximal motor axons and the recovery of muscle function after the second stage of surgery. Further research into how phenotype, gene expression and changes in neurotrophic factors in SCs are affected by GDNF will help us design more effective methods to treat peripheral nerve injury.

Acknowledgements

This research was funded in part by the following:

National Science Foundation for Young Scientists of China (Grant No. 81702168).

Fujian Youth Development Programme of NHC (Grant No. 2018-ZQN-31).

Fujian Science Foundation Youth Innovation Project (Grant No. 2018J05138).

References

Abdullah, M., O'Daly, A., Vyas, A., Rohde, C., Brushart, T.M., 2013. Adult motor axons preferentially reinnervate predegenerated muscle nerve. Exp. Neurol. 249, 1–7.

Blits, B., Carlstedt, T.P., Ruitenberg, M.J., de Winter, F., Hermens, W.T., Dijkhuizen, P.A., Claasens, J.W.C., Eggers, R., van der Sluis, R., Tenenbaum, L., 2004. Rescue and sprouting of motoneurons following ventral root avulsion and reimplantation combined with intraspinal adeno-associated viral vector-mediated expression of glial cell line-derived neurotrophic factor or brain-derived neurotrophic factor. Exp. Neurol. 189, 303–316.

Brenner, M.J., Hess, J.R., Myckatyn, T.M., Hayashi, A., Hunter, D.A., Mackinnon, S.E., 2006. Repair of motor nerve gaps with sensory nerve inhibits regeneration in rats. Laryngoscope 116, 1685–1692.

Brushart, T.M., 1988. Preferential reinnervation of motor nerves by regenerating motor axons. J. Neurosci. 8, 1026–1031.

Brushart, T.M., Aspalter, M., Griffin, J.W., Redett, R., Hameed, H., Zhou, C., Wright, M., Vyas, A., Höke, A., 2013. Schwann cell phenotype is regulated by axon modality and central–peripheral location, and persists in vitro. Exp. Neurol. 247, 272–281.

Chu, T.-H.H., Du, Y., Wu, W., 2008. Motor nerve graft is better than sensory nerve graft for survival and regeneration of motoneurons after spinal root avulsion in adult rats. Exp. Neurol. 212, 562–565.

Chu, T.-H., Li, S.-Y., Guo, A., Wong, W.-M., Yuan, Q., Wu, W., 2009. Implantation of neurotrophic factor-treated sensory nerve graft enhances survival and axonal regeneration of motoneurons after spinal root avulsion. J. Neuropathol. Exp. Neurol. 68, 94–101.

Eggers, R., Tannemaat, M.R., Winter, F. De, Malessy, M.J.A., Verhaagen, J., 2016. Clinical and neurobiological advances in promoting regeneration of the ventral root avulsion lesion. 43, 318–335.

Fang, X., Zhang, W., Zhang, C., Wong, W., Li, W., Wu, W., Lin, J., 2016. Lithium accelerates functional motor recovery by improving Remyelination of regenerating axons following ventral root avulsion and Reimplantation. Neuroscience 329, 213–225.

Gao, M., Lu, P., Lynam, D., Bednark, B., Campana, W.M., Sakamoto, J., Tuszynski, M., 2016. BDNF gene delivery within and beyond templated agarose multi-channel guidance scaffolds enhances peripheral nerve regeneration. J. Neural Eng. 13, 66011.

Gordon, T., 2014. Neurotrophic factor expression in denervated motor and sensory Schwann cells: relevance to specificity of peripheral nerve regeneration. Exp. Neurol. 254, 99–108.

Gordon, T., Tyreman, N., Raji, M.A., 2011. The basis for diminished functional recovery after delayed peripheral nerve repair. J. Neurosci. 31, 5325–5334.

Griffin, J.W., Hogan, M.V., Chhabra, A.B., Deal, D.N., 2013. Peripheral nerve repair and reconstruction. JBJS 95, 2144–2151.

de Groot, D.M., Coenen, A.J.M., Verhofstad, A., van Herp, F., Martens, G.J.M., Dorien, M. de G., Anton, J.M.C., Albert, V., François van, H., Gerard, J.M.M., 2006. In vivo induction of glial cell proliferation and axonal outgrowth and myelination by brain-derived neurotrophic factor. Mol. Endocrinol. 20, 2987–2998.

Gu, H.-Y., Chai, H., Zhang, J.-Y., Yao, Z.-B., Zhou, L.-H., Wong, W.-M., Bruce, I.C., Wu, W.-T., 2005. Survival, regeneration and functional recovery of motoneurons after

delayed reimplantation of avulsed spinal root in adult rat. Exp. Neurol. 192, 89–99.
Guo, J., Leung, K.K.G., Su, H., Yuan, Q., Wang, L., Chu, T.H., Zhang, W., Pu, J.K.S., Ng, G.K.P., Wong, W.M., Dai, X., Wu, W., 2009. Self-assembling peptide nanofiber scaffold promotes the reconstruction of acutely injured brain. Nanomedicine Nanotechnology, Biol. Med. 5, 345–351.
Höke, A., Gordon, T., Zochodne, D.W., Sulaiman, O.A.R., 2002. A decline in glial cell-line-derived neurotrophic factor expression is associated with impaired regeneration after long-term Schwann cell denervation. Exp. Neurol. 173, 77–85.
Höke, A., Ho, T., Crawford, T.O., LeBel, C., Hilt, D., Griffin, J.W., 2003. Glial cell line-derived neurotrophic factor alters axon schwann cell units and promotes myelination in unmyelinated nerve fibers. J. Neurosci. 23, 561–567.
Höke, A., Redett, R., Hameed, H., Jari, R., Zhou, C., Li, Z.B., Griffin, J.W., Brushart, T.M., 2006. Schwann cells express motor and sensory phenotypes that regulate axon regeneration. J. Neurosci. 26, 9646–9655.
Hu, J., Zhu, Q.-T., Liu, X.-L., Xu, Y., Zhu, J.-K., 2007. Repair of extended peripheral nerve lesions in rhesus monkeys using acellular allogenic nerve grafts implanted with autologous mesenchymal stem cells. Exp. Neurol. 204, 658–666.
Huang, J., Lu, L., Zhang, J., Hu, X., Zhang, Y., Liang, W., Wu, S., Luo, Z., 2012. Electrical stimulation to conductive scaffold promotes axonal regeneration and remyelination in a rat model of large nerve defect. PLoS One 7, e39526.
Iwase, T., Jung, C.G., Bae, H., Zhang, M., Soliven, B., 2005. Glial cell line-derived neurotrophic factor-induced signaling in Schwann cells. J. Neurochem. 94, 1488–1499.
Jesuraj, N.J., Nguyen, P.K., Wood, M.D., Moore, A.M., Borschel, G.H., Mackinnon, S.E., Sakiyama-Elbert, S.E., 2012. Differential gene expression in motor and sensory Schwann cells in the rat femoral nerve. J. Neurosci. Res. 90, 96–104.
Jesuraj, N.J., Marquardt, L.M., Kwasa, J.A., Sakiyama-Elbert, S.E., 2014. Glial cell line-derived neurotrophic factor promotes increased phenotypic marker expression in femoral sensory and motor-derived Schwann cell cultures. Exp. Neurol. 257, 10–18.
Jonsson, S., Wiberg, R., McGrath, A.M., Novikov, L.N., Wiberg, M., Novikova, L.N., Kingham, P.J., 2013. Effect of delayed peripheral nerve repair on nerve regeneration, Schwann cell function and target muscle recovery. PLoS One 8, e56484.
Kawamura, D.H., Johnson, P.J., Moore, A.M., Magill, C.K., Hunter, D.A., Ray, W.Z., Tung, T.H.H., Mackinnon, S.E., 2010. Matching of motor-sensory modality in the rodent femoral nerve model shows no enhanced effect on peripheral nerve regeneration. Exp. Neurol. 223, 496–504.
Kehoe, S., Zhang, X.F., Boyd, D., 2012. FDA approved guidance conduits and wraps for peripheral nerve injury: a review of materials and efficacy. Injury 43, 553–572.
Koutsopoulos, S., Unsworth, L.D., Nagai, Y., Zhang, S., 2009. Controlled release of functional proteins through designer self-assembling peptide nanofiber hydrogel scaffold. Proc. Natl. Acad. Sci. 106, 4623–4628.
Liu, Y., Grumbles, R.M., Thomas, C.K., 2013. Electrical stimulation of embryonic neurons for 1 hour improves axon regeneration and the number of reinnervated muscles that function. J. Neuropathol. Exp. Neurol. 72, 697–707.
Lohmeyer, J.A., Siemers, F., Machens, H.-G., Mailänder, P., 2009. The clinical use of artificial nerve conduits for digital nerve repair: a prospective cohort study and literature review. J. Reconstr. Microsurg. 25, 55–61.
Madison, R.D., Sofroniew, M.V., Robinson, G.A., 2009. Schwann cell influence on motor neuron regeneration accuracy. Neuroscience 163, 213–221.
Marquardt, L.M., Sakiyama-Elbert, S.E., 2015. GDNF preconditioning can overcome Schwann cell phenotypic memory. Exp. Neurol. 265, 1–7.
Marquardt, L.M., Ee, X., Iyer, N., Hunter, D., Mackinnon, S.E., Wood, M.D., Sakiyama-Elbert, S.E., 2015. Finely tuned temporal and spatial delivery of GDNF promotes enhanced nerve regeneration in a long nerve defect model. Tissue Eng. Part A 21, 2852–2864.
Mears, S., Schachner, M., Brushart, T.M., 2003. Antibodies to myelin-associated glycoprotein accelerate preferential motor reinnervation. J. Peripher. Nerv. Syst. 8, 91–99.
Michalski, B., Bain, J.R., Fahnestock, M., 2008. Long-term changes in neurotrophic factor expression in distal nerve stump following denervation and reinnervation with motor or sensory nerve. J. Neurochem. 105, 1244–1252.
Neubauer, D., Graham, J.B., Muir, D., 2010. Nerve grafts with various sensory and motor fiber compositions are equally effective for the repair of a mixed nerve defect. Exp. Neurol. 223, 203–206.
Raff, M.C., Abney, E., Brockes, J.P., Hornby-Smith, A., 1978. Schwann cell growth factors. Cell 15, 813–822.
Rosenberg, S.S., Ng, B.K., Chan, J.R., 2006. The quest for remyelination: a new role for neurotrophins and their receptors. Brain Pathol. 16, 288–294.
Schäfer, M., Fruttiger, M., Montag, D., Schachner, M., Martini, R., 1996. Disruption of the gene for the myelin-associated glycoprotein improves axonal regrowth along myelin in C57BL/WId(s) mice. Neuron 16, 1107–1113.
Sun, Y., Li, W., Wu, X., Zhang, N., Zhang, Y., Ouyang, S., Song, X., Fang, X., Seeram, R., Xue, W., 2016. Functional self-assembling peptide nanofiber hydrogels designed for nerve degeneration. ACS Appl. Mater. Interfaces 8, 2348–2359.
Wallquist, W., Zelano, J., Plantman, S., Kaufman, S.J., Cullheim, S., Hammarberg, H., 2004. Dorsal root ganglion neurons up-regulate the expression of laminin-associated integrins after peripheral but not central axotomy. J. Comp. Neurol. 480, 162–169.
Wood, M.D., Moore, A.M., Hunter, D.A., Tuffaha, S., Borschel, G.H., Mackinnon, S.E., Sakiyama-Elbert, S.E., 2009. Affinity-based release of glial-derived neurotrophic factor from fibrin matrices enhances sciatic nerve regeneration. Acta Biomater. 5, 959–968.
Xue, C., Hu, N., Gu, Y., Yang, Y., Liu, Y., Liu, J., Ding, F., Gu, X., 2012. Joint use of a chitosan/PLGA scaffold and MSCs to bridge an extra large gap in dog sciatic nerve. Neurorehabil. Neural Repair 26, 96–106.
Zhan, X., Gao, M., Jiang, Y., Weiwei, Zhang, Wong, W.M., Yuan, Q., Su, H., Kang, X., Dai, X., Wenying, Zhang, Guo, J., Wu, W., 2013. Nanofiber scaffolds facilitate functional regeneration of peripheral nerve injury. Nanomedicine Nanotechnology, Biol. Med. 9, 305–315.
Zhang, L., Ma, Z., Smith, G.M., Wen, X., Pressman, Y., Wood, P.M., Xu, X., 2009. GDNF-enhanced axonal regeneration and myelination following spinal cord injury is mediated by primary effects on neurons. Glia 57, 1178–1191.
Zhang, W., Fang, X., Zhang, C., Li, W., Wong, W.M., Xu, Y., Wu, W., Lin, J., 2017. Transplantation of embryonic spinal cord neurons to the injured distal nerve promotes axonal regeneration after delayed nerve repair. Eur. J. Neurosci. 45, 750–762.